627 **Supplemental Information**
628

629 **Title: ESCRT recruitment to mRNA-encoded SARS-CoV-2 spike induces virus-**
630 **like particles and enhanced antibody responses**

631

632 **Authors:** Magnus A. G. Hoffmann[1*], Zhi Yang[1‡], Kathryn E. Huey-Tubman[1],
633 Alexander A. Cohen[1], Priyanthi N. P. Gnanapragasam[1], Leesa M. Nakatomi[1], Kaya
634 N. Storm[1], Woohyun J. Moon[2], Paulo J.C. Lin[2], Pamela J. Bjorkman[1*]

635

636 **Affiliations:**
637 [1]Division of Biology and Biological Engineering, California Institute of Technology,
638 Pasadena, CA 91125, USA
639 [2]Acuitas Therapeutics, Vancouver, BC, V6T 1Z3, CANADA
640 ‡Present address: Department of Molecular and Cell Biology, University of California,
641 Berkeley, CA 94720, USA

642

643 [*]To whom correspondence should be addressed: Email: mhoffman@caltech.edu,
644 bjorkman@caltech.edu

645

646

Methods

Design of EABR constructs

The EABR domain (residues 160-217) of the human CEP55 protein was fused to the C-terminus of the SARS-CoV-2 S protein (WA1/D614G) separated by a 4-residue $(Gly)_3Ser$ (GS) linker to generate S-EABR/no EPM. This construct contained the native furin cleavage site, 2P stabilizing mutations (Pallesen et al., 2017), and the C-terminal 21 residues were truncated to remove an ER-retention signal (McBride et al., 2007). The S-EABR construct was generated by inserting residues 243-290 of mouse FcgRII-B1 upstream of the 4-residue GS linker and the EABR domain. The S-$EABR_{min1}$ and S-$EABR_{min2}$ constructs encoded residues 170-217 and 170-208 of CEP55, respectively. EABR constructs were also generated for HIV-1 Env_{YU2} and human CCR5. S-p6, S-$VP40_{1-44}$, and S-p9 were generated by replacing the EABR domain gene with sequences encoding HIV-1 p6 (isolate HXB2), EBOV VP40 (residues 1-44; Zaire EBOV), and EIAV p9 (strain Wyoming), respectively. The S-ferritin construct was designed as described (Powell et al., 2021) by fusing genes encoding the ectodomain of SARS-CoV-2 S WA1/D614G containing a furin cleavage site and 2P mutations, and *Helicobacter pylori* ferritin, separated by a 3-residue Ser-Gly-Gly linker. All constructs were cloned into the p3bNC expression plasmid.

Production of EABR eVLPs

EABR eVLPs were generated by transfecting Expi293F cells (Gibco) cultured in Expi293F expression media (Gibco) on an orbital shaker at 37°C and 8% CO_2. Gag-based eVLPs were produced by co-transfecting Expi293F cells with a plasmid expressing Rev-independent HIV-1 Gag-Pol (pHDM-Hgpm2 plasmid; PlasmID Repository, Harvard Medical School) and SARS-CoV-2 S, HIV-1 Env_{YU2}, or CCR5,

672 respectively, at a ratio of 1:1. SARS-CoV-2 M/N/E-based eVLPs were produced by
673 co-transfecting Expi293F cells with plasmids expressing the SARS-CoV-2 M, N, E,
674 and S proteins at a ratio of 1:1:1:1. To enable interactions between M, N, E, and S,
675 we transfected full-length S with an untruncated cytoplasmic domain. 72 hours post-
676 transfection, cells were centrifuged at 400 x g for 10 min, supernatants were passed
677 through a 0.45 µm syringe filter and concentrated using Amicon Ultra-15 centrifugal
678 filters with 100 kDa molecular weight cut-off (Millipore). eVLPs were purified by
679 ultracentrifugation at 50,000 rpm (135,000 x g) for 2 hours at 4°C using a TLA100.3
680 rotor and a Optima^{TM} TLX ultracentrifuge (Beckman Coulter) on a 20% w/v sucrose
681 cushion. Supernatants were removed and pellets were re-suspended in 200 µL sterile
682 PBS at 4°C overnight. To remove residual cell debris, samples were centrifuged at
683 10,000 x g for 10 min and supernatants were collected. For in vivo studies and cryo-
684 ET, eVLPs were further purified by SEC using a Superose 6 10/300 column (GE
685 Healthcare) equilibrated with PBS. Peak fractions corresponding to S-EABR eVLPs
686 were combined and concentrated to 250-500 µL in Amicon Ultra-4 centrifugal filters
687 with 100 kDa molecular weight cut-off. Samples were aliquoted and stored at -20°C.
688
689 **Protein expression**
690 Soluble SARS-CoV-2 S-6P trimers (WA1/D614G) (Hsieh et al., 2020) and RBDs were
691 expressed as described (Cohen et al., 2022; Wang et al., 2022). Briefly, Avi/His-
692 tagged proteins were purified from transiently-transfected Expi293F cells (Gibco) by
693 nickel affinity chromatography and SEC (Barnes et al., 2020; Cohen et al., 2022; Wang
694 et al., 2022). Peak fractions corresponding to S-6P or RBD proteins were pooled,
695 concentrated, and stored at 4ºC. Biotinylated proteins for ELISAs were generated by
696 co-transfection of Avi/His-tagged S-6P and RBD constructs with a plasmid encoding

an endoplasmic reticulum-directed BirA enzyme (kind gift from Michael Anaya, Caltech). S-6P constructs with a C-terminal SpyTag003 tag (Keeble et al., 2019) were expressed for covalent coupling to a 60-mer protein nanoparticle (SpyCatcher003-mi3) using the SpyCatcher-SpyTag system (Brune et al., 2016; Zakeri et al., 2012).

Preparation of SpyCatcher003-mi3 nanoparticles

SpyCatcher003-mi3 (Cohen et al., 2021) displaying SpyTagged SARS-CoV-2 S-6P trimers were prepared as described (Cohen et al., 2021; Cohen et al., 2022). Briefly, SpyCatcher003-mi3 subunits with N-terminal 6xHis tags were expressed in BL21 (DE3)-RIPL *E. coli* (Agilent). Bacterial cell pellets were lysed using a cell disruptor in the presence of 2.0 mM PMSF (Sigma). Lysates were centrifuged at 21,000 x g for 30 min, and supernatants were collected and filtered through a 0.2 µm filter. SpyCatcher003-mi3 was purified by Ni-NTA chromatography using a pre-packed HisTrap™ HP column (GE Healthcare), concentrated in Amicon Ultra-15 centrifugal filters with 30 kDa molecular weight cut-off (Millipore), and purified by SEC on a HiLoad 16/600 Superdex 200 column (GE Healthcare) equilibrated with TBS. S-mi3 nanoparticles were generated by incubating purified SpyCatcher003-mi3 with a 3-fold molar excess of purified SpyTagged S-6P trimer overnight at 4ºC in TBS. Conjugated S-mi3 nanoparticles were separated from uncoupled S-6P trimers by SEC using a Superose 6 10/300 column (GE Healthcare) equilibrated with PBS. Fractions corresponding to conjugated S-mi3 were identified by sodium dodecyl sulfate polyacrylamide gel electrophoresis (SDS-PAGE) and pooled.

722 **Western blot analysis**

723 The presence of SARS-CoV-2 S, HIV-1 Env_{YU2}, and CCR5 on purified eVLPs was
724 detected by Western blot analysis. Samples were diluted in SDS-PAGE loading buffer
725 under reducing conditions, separated by SDS-PAGE, and transferred to nitrocellulose
726 membranes (0.2 µm) (GE Healthcare). The following antibodies were used for
727 detecting SARS-CoV-2 S, HIV-1 Env_{YU2}, and CCR5: rabbit anti-SARS-CoV-2 S1
728 protein (PA5-81795; ThermoFisher) at 1:2,500, the human anti-HIV-1 Env broadly
729 neutralizing antibody 10-1074 (Mouquet et al., 2012) (expressed in-house) at
730 1:10,000, rat anti-CCR5 (ab111300; Abcam) at 1:2,000, HRP-conjugated mouse anti-
731 rabbit IgG (211-032-171; Jackson ImmunoResearch) at 1:10,000, HRP-conjugated
732 goat anti-human IgG (2014-05; Southern Biotech) at 1:8,000, and HRP-conjugated
733 mouse anti-rat IgG (3065-05; Southern Biotech) at 1:10,000. Protein bands were
734 visualized using ECL Prime Western Blotting Detection Reagent (GE Healthcare).
735
736 For in vivo studies, the amount of SARS-CoV-2 S on S-EABR eVLPs was determined
737 by quantitative Western blot analysis. Various dilutions of SEC-purified S-EABR eVLP
738 samples and known amounts of soluble SARS-CoV-2 S1 protein (Sino Biological)
739 were separated by SDS-PAGE and transferred to nitrocellulose membranes (GE
740 Healthcare). SARS-CoV-2 S was detected as described above. Band intensities of the
741 SARS-CoV-2 S1 standards and S-EABR eVLP sample dilutions were measured using
742 ImageJ to determine S concentrations. The S1 protein concentrations determined for
743 S-EABR samples were multiplied by a factor of 1.8 to account for the difference in
744 molecular weight between S1 and the full-length S protein.
745
746

747 **Cryo-ET of S-EABR eVLPs**

748 SEC-purified S-EABR eVLPs were prepared on grids for cryo-ET using a Mark IV
749 Vitrobot (ThermoFisher Scientific) operated at 21°C and 100% humidity. 2.5 µL of
750 sample was mixed with 0.4 µL of 10 nm fiducial gold beads (Sigma-Aldrich) and
751 applied to 300-mesh Quantifoil R2/2 grids, blotted for 3.5 s, and then plunge-frozen in
752 liquid ethane cooled by liquid nitrogen. Image collections were performed on a 300 kV
753 Titan Krios transmission electron microscope (ThermoFisher Scientific) operating at a
754 nominal 42,000x magnification. Tilt series were collected on a K3 direct electron
755 detector (Gatan) with a pixel size of 2.15 Å•pixel^{-1} using SerialEM software
756 (Mastronarde, 2005). The defocus range was set to -5 to -8 µm and a total of 120 e^- •
757 Å^{-2} per tilt series. Images were collected using a dose-symmetric scheme (Hagen et
758 al., 2017) ranging from -60° to 60° with 3° intervals. Tomograms were aligned and
759 reconstructed using IMOD (Mastronarde and Held, 2017).
760
761 To build a model of an S-EABR eVLP, coordinates of a SARS-CoV-2 S trimer (PDB
762 6VXX) were fit into spike densities in the reconstructed tomograms using ChimeraX
763 (Goddard et al., 2018). Positions and orientations of the S protein were adjusted in a
764 hemisphere of the eVLP in which the spike density was of higher quality. A 55 nm
765 sphere was adapted from a cellPACK model (cellPACK ID: HIV-1_0.1.6_6) (Johnson
766 et al., 2015; Johnson et al., 2014) and added to the model to represent the eVLP
767 membrane surface.
768
769 **Neutralization assays**
770 Lentivirus-based SARS-CoV-2 pseudoviruses were generated as described
771 (Crawford et al., 2020; Robbiani et al., 2020) using S proteins from the WA1/D614G,

772 Delta, Omicron BA.1, Omicron BA.2, and Omicron BA.4/5 variants in which the C-
773 terminal 21 residues of the S protein cytoplasmic tails were removed (Crawford et al.,
774 2020). Serum samples from immunized mice were heat-inactivated for 30 min at 56ºC.
775 Three-fold serial dilutions of heat-inactivated samples were incubated with
776 pseudoviruses for 1 hour at 37ºC, followed by addition of the serum-virus mixtures to
777 pre-seeded HEK293T-ACE2 target cells. After 48-hour incubation at 37ºC, BriteLite
778 Plus substrate (Perkin Elmer) was added and luminescence was measured. Half-
779 maximal inhibitory dilutions (ID_{50}s) were calculated using 4-parameter non-linear
780 regression analysis in AntibodyDatabase (West et al., 2013) and ID_{50} values were
781 rounded to three significant figures.
782
783 $PRNT_{50}$ (50% plaque reduction neutralization test) assays with authentic SARS-CoV-
784 2 virus were performed in a biosafety level 3 facility at BIOQUAL, Inc. (Rockville, MD)
785 as described (Haun et al., 2020). Mouse sera from day 56 post-immunization were
786 diluted 1:20 and then 3-fold serially diluted in culture media (DMEM + 10% FBS +
787 Gentamicin). The diluted samples were incubated with 30 plaque-forming units of wild-
788 type SARS-CoV-2 (USA-WA1/2020, BEI Resources NR-52281; Beta variant, Isolate
789 hCoV-19/South Africa/KRISP-K005325/2020, BEI Resources NR-54009; Delta
790 variant, isolate hCoV-19/USA/MD-HP05647/2021 BEI Resources NR-55674) for 1
791 hour at 37ºC. Samples were then added to a confluent monolayer of Vero/TMPRSS2
792 cells in 24-well plates for 1 hour at 37ºC in 5% CO_2. 1 mL of culture media with 0.5%
793 methylcellulose was added to each well and plates were incubated for 3 days at 37ºC
794 in 5% CO_2. Plates were fixed with ice cold methanol at -20ºC for 30 min. Methanol
795 was discarded and plates were stained with 0.2% crystal violet for 30 min at room
796 temperature. Plates were washed once with water and plaques in each well were

797 counted. $TCID_{50}$ values were calculated using the Reed-Muench formula (Reed and
798 Muench, 1938).
799
800 **ELISAs**
801 Pre-blocked streptavidin-coated Nunc® MaxiSorp™ 384-well plates (Sigma) were
802 coated with 5 µg/mL biotinylated S-6P or RBD proteins in Tris-buffered saline with
803 0.1% Tween 20 (TBS-T) and 3% bovine serum albumin (BSA) for 1 hour at room
804 temperature. Serum samples from immunized mice were diluted 1:100, 4-fold serially
805 diluted in TBS-T/3% BSA, and then added to plates. After a 3-hour incubation at room
806 temperature, plates were washed with TBS-T using an automated plate washer. HRP-
807 conjugated goat anti-mouse IgG (715-035-150; Jackson ImmunoResearch) was
808 diluted 1:100,000 in TBS-T/3% BSA and added to plates for 1 hour at room
809 temperature. After washing with TBS-T, plates were developed using SuperSignal™
810 ELISA Femto Maximal Signal Substrate (ThermoFisher) and absorbance was
811 measured at 425 nm. Area under the curve (AUC) calculations for binding curves were
812 performed using GraphPad Prism 9.3.1 assuming a one-site binding model with a Hill
813 coefficient as described (Cohen et al., 2021).
814
815 **mRNA synthesis**
816 Codon-optimized mRNAs encoding SARS-CoV-2 S, S-EPM, S-EABR/no EPM, and
817 S-EABR constructs were synthesized by RNAcore
818 (https://www.houstonmethodist.org/research-cores/rnacore/) using proprietary
819 manufacturing protocols. mRNAs were generated by T7 RNA polymerase-mediated
820 in vitro transcription reactions using DNA templates containing the immunogen open
821 reading frame flanked by 5′ untranslated region (UTR) and 3′ UTR sequences and

terminated by an encoded polyA tail. CleanCap 5' cap structures (TriLink) were incorporated into the 5′ end co-transcriptionally. Uridine was completely replaced with N1-methyl-pseudouridine to reduce immunogenicity (Kariko et al., 2008). mRNAs were purified by oligo-dT affinity purification and high-performance liquid chromatography (HPLC) to remove double-stranded RNA contaminants (Kariko et al., 2011). Purified mRNAs were stored at –80 °C.

mRNA transfections

For mRNA transfections, 10^6 HEK293T cells were seeded in 6-well plates. After 24 hours, cells were transfected with 2 µg mRNA encoding SARS-CoV-2 S, S-EPM, S-EABR/no EPM, or S-EABR constructs using Lipofectamine™ MessengerMax™ transfection reagent (ThermoFisher). 48 hours post-transfection, supernatants were collected and purified for Western blot analysis. Cells were gently detached by pipetting and resuspended in 500 µL PBS. 100 µL were transferred into Eppendorf tubes for flow cytometry analysis of S cell surface expression. Cells were stained with the SARS-CoV-2 antibody C119 (Robbiani et al., 2020) at 5 µg/mL in PBS+ (PBS supplemented with 2% FBS) for 30 min at room temperature in the dark. After two washes in PBS+, samples were stained with an Alexa Fluor® 647-conjugated anti-human IgG secondary antibody (A21445; Life Technologies) at a 1:2,000 dilution in PBS+ for 30 min at room temperature in the dark. After two washes in PBS+, cells were resuspended in PBS+ and analyzed by flow cytometry (MACSQuant, Miltenyi Biotec). Results were plotted using FlowJo 10.5.3 software.

847 **LNP encapsulation of mRNAs**

848 Purified N1-methyl-pseudouridine mRNA was formulated in LNP as previously
849 described (Pardi et al., 2015). In brief, 1,2-distearoyl-*sn*-glycero-3-phosphocholine,
850 cholesterol, a PEG lipid, and an ionizable cationic lipid dissolved in ethanol were
851 rapidly mixed with an aqueous acidic solution containing mRNA using an in-line mixer.
852 The ionizable lipid and LNP composition are described in the international patent
853 application WO2017075531(2017). The post in-line solution was dialyzed with PBS
854 to remove the ethanol and displace the acidic solution. Subsequently, LNP was
855 measured for size (60-65 nm) and polydispersity (PDI < 0.075) by dynamic light
856 scattering (Malvern Nano ZS Zetasizer). Encapsulation efficiencies were >97% as
857 measured by the Quant-iT Ribogreen Assay (Life Technologies).

858

859 **Immunizations**

860 All animal procedures were performed in accordance with IACUC-approved protocols.
861 7-8 week-old female C57BL/6 or BALB/c mice (Charles River Laboratories) were used
862 for immunization experiments with cohorts of 8-10 animals per group. 0.1 μg of protein-
863 based immunogens, including soluble S trimer, S-mi3, and purified S-EABR eVLPs,
864 were administered to C57BL/6 mice by subcutaneous (SC) injections on days 0 and
865 28 in the presence of Sigma adjuvant system (Sigma). 2 μg of S and S-EABR mRNA-
866 LNP were administered to BALB/c mice by intramuscular (IM) injections on days 0 and
867 28. To compare mRNA- and protein-based immunogens, 1 μg purified S-EABR eVLPs
868 were administered IM in the presence of 50% v/v AddaVax^{TM} adjuvant (Invivogen).
869 Serum samples for ELISAs and neutralization assays were obtained on indicated
870 days.

871

872 **ELISpot assays**

873 Animals were euthanized on day 112 and spleens were collected. Spleens were
874 homogenized using a gentleMACS Octo Dissociator (Miltenyi Biotec). Cells were
875 passed through a 70 µm tissue screen, centrifuged at 1,500 rpm for 10 min, and
876 resuspended in CTL-Test™ media (ImmunoSpot) containing 1% GlutaMAX™ (Gibco)
877 for ELISpot analysis to evaluate T cell responses. A PepMix™ pool of 315 peptides
878 (15-mers with 11 amino acid overlap) derived from the SARS-CoV-2 S protein (JPT
879 Peptide Technologies) was added to mouse IFN-g/IL-4 double-color ELISpot plates
880 (ImmunoSpot) at a concentration of 2 µg/mL. 300,000 cells were added per well, and
881 plates were incubated at 37ºC for 24 hours. Biotinylated detection, streptavidin-
882 alkaline phosphatase (AP), and substrate solutions were added according to the
883 manufacturer's guidelines. Plates were gently rinsed with water three times to stop the
884 reactions. Plates were air-dried for two hours in a running laminar flow hood. The
885 number of spots and the mean spot sizes were quantified using a CTL ImmunoSpot
886 S6 Universal-V Analyzer (Immunospot).

887

888 **Statistical analysis**

889 Titer differences between immunized groups of mice for ELISAs and neutralization
890 assays were evaluated for statistical significance using the non-parametric Kruskal-
891 Wallis test followed by Dunn's multiple comparison post hoc test calculated using
892 Graphpad Prism 9.3.1. For ELISpot results, statistically significant differences
893 between immunized groups of mice were determined using analysis of variance
894 (ANOVA) test followed by Tukey's multiple comparison post hoc test calculated using
895 Graphpad Prism 9.3.1.

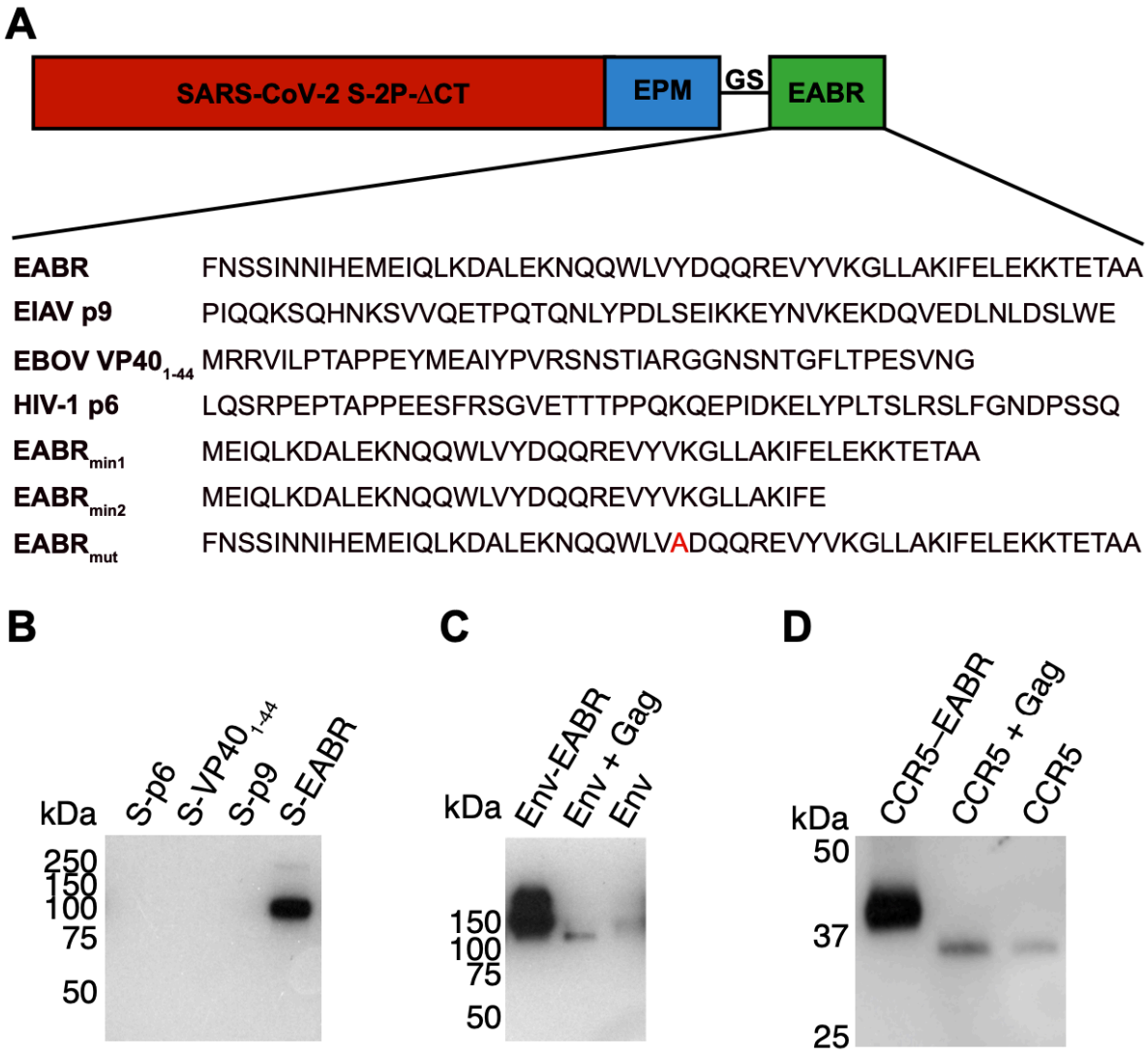

Figure S1 Comparison of EABR-related sequence insertions in the cytoplasmic tail of SARS-CoV-2 S, related to Figure 1.

(A) Top: Schematic of different S-EABR constructs that were compared for their ability to induce eVLP assembly. EPM = Endocytosis prevention motif. GS = $(Gly)_3Ser$ linker. EABR = ESCRT- and ALIX-binding region. Bottom: Amino acid sequences of EABR portion of different constructs.

(B) Western blot analysis of SARS-CoV-2 S1 protein levels on eVLPs purified by ultracentrifugation on a 20% sucrose cushion from transfected Expi293F cell culture

906 supernatants. Cells were transfected with S-p6, S-VP40$_{1-44}$, S-p9, or S-EABR
907 constructs. Purified eVLP samples were diluted 1:400.
908
909 (C) Western blot analysis comparing HIV-1 Env$_{YU2}$ levels in eVLP samples purified
910 from transfected Expi293F cell culture supernatants. Cells were transfected with
911 plasmids encoding Env-EABR, Env plus HIV-1 Gag, or Env alone. Purified eVLP
912 samples were diluted 1:200.
913
914 (D) Western blot analysis comparing CCR5 levels in eVLP samples purified from
915 transfected Expi293F cell culture supernatants. Cells were transfected with plasmids
916 encoding CCR5-EABR, CCR5 plus HIV-1 Gag, or CCR5 alone. Purified eVLP
917 samples were diluted 1:200. The migration difference between CCR5-EABR and
918 CCR5 is due to addition of the EABR sequence (~7 kDa) that increases its molecular
919 mass.

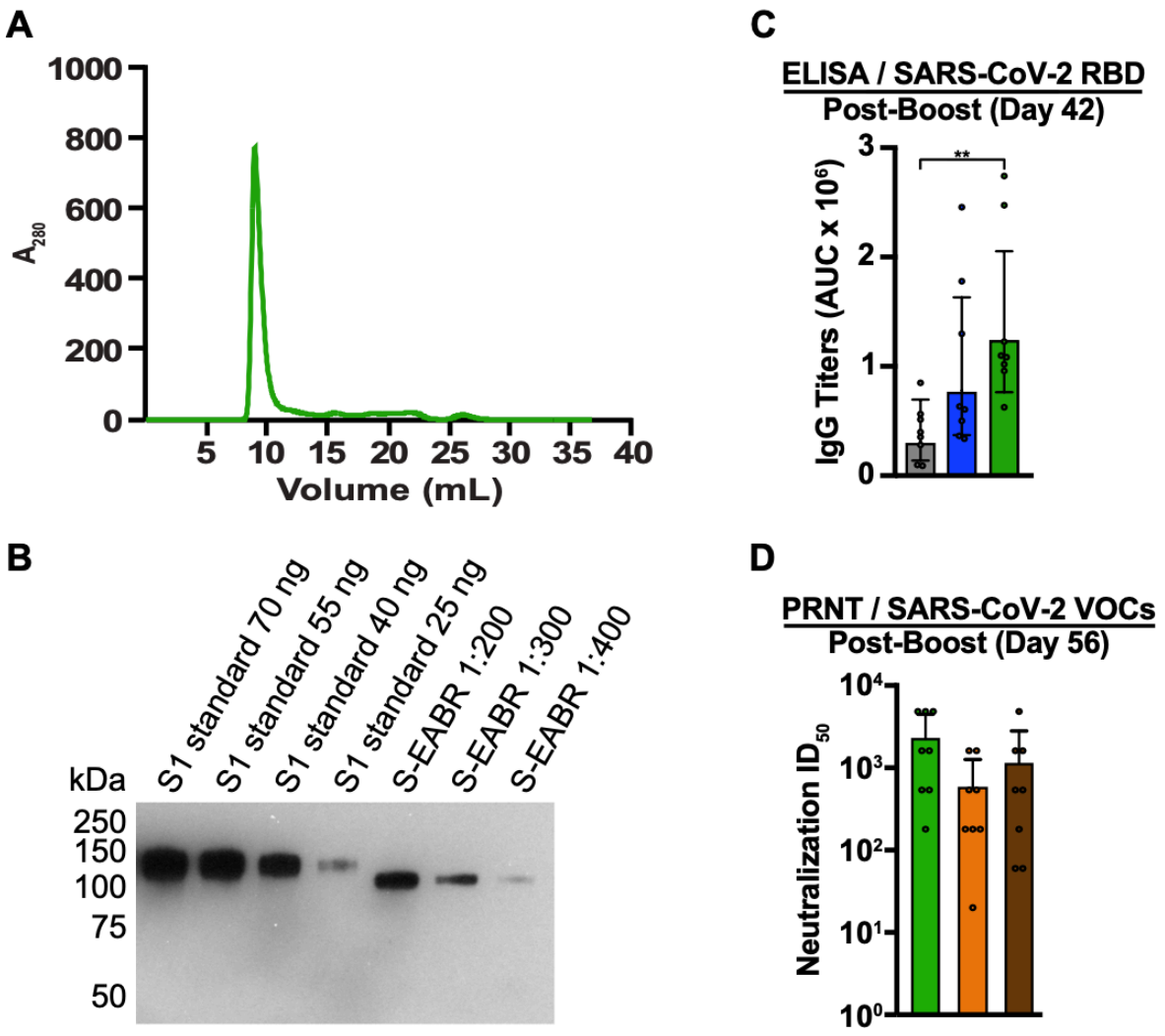

Figure S2 Purified S-EABR eVLPs induce potent antibody responses in mice, related to Figure 2.

(A) Size exclusion chromatogram of S-EABR eVLPs purified by ultracentrifugation on a 20% sucrose cushion.

(B) Quantitative Western blot comparing indicated amounts of SARS-CoV-2 S1 standards (lanes 1-4) and various dilutions of purified S-EABR eVLPs (lanes 5-7) to determine S protein concentrations in eVLP samples. The S1 standard protein (Sino Biological) was biotinylated and contained a polyhistidine tag, which resulted in a difference in apparent molecular weights for the S1 standards and the S-EABR

construct. Band intensities of S1 standards and S-EABR eVLP sample dilutions were measured using ImageJ to determine S concentrations.

(C) ELISA data from day 42 for antisera from individual mice (colored circles) immunized with soluble S (purified S trimer) (gray), S-mi3 (S trimer ectodomains covalently attached to mi3, a 60-mer protein nanoparticle) (blue), or S-EABR eVLPs (green). Results are shown as area under the curve (AUC) and presented as the geometric mean (bars) and standard deviation (horizontal lines). Significant differences between cohorts linked by horizontal lines are indicated by asterisks: $p<0.05$ = *, $p<0.01$ = **.

(D) PRNT assay results from day 56 for antisera from individual mice (colored circles) immunized with S-EABR eVLPs. Results against the SARS-CoV-2 WA1 (green), Beta (orange), and Delta (brown) variants are shown as $TCID_{50}$ values (Reed and Muench, 1938) and presented as the geometric mean (bars) and standard deviation (horizontal lines).